# Droplets emission from FEEP and colloids thrusters: modelling of droplets dynamics and interaction with spacecraft body

**IEPC-2019-196**

*Presented at the 36th International Electric Propulsion Conference*
*University of Vienna • Vienna, Austria*
*September 15-20, 2019*

M. Villemant[1], P. Sarrailh[1] and S. Hess[1]
ONERA - The French Aerospace Lab, Toulouse, France

**Abstract:**

## Nomenclature

SPIS = Spacecraft Plasma Interaction System
FEEP = Field Electron Emission Propulsion

## I. FEEP and colloid thrusters technology, context of development

FEEP and colloids thrusters are two electric propulsion technologies which experience a growth of interest since a few years. This is essentially due to some of their characteristics which make them interesting for scientific and commercial missions. FEEP and colloids thrusters are characterized by high specific impulse, low thrust, good compactness and a low total mass. The data presented in Table 1 have been measured on the FEEP thruster In-FEEP which was planned to fly on LISA-Pathfinder mission.

**Table 1 : In-FEEP thruster characteristics**

| | |
|---|---|
| **Specific impulse** | 1600-8000 s |
| **Thrust** | 0.1-100 µN |
| **Total thruster mass** | 2.5 Kg |
| **Total power supply** | 13 W |

These characteristics make FEEP and colloids technologies highly interesting for several scientific missions where precise satellites or probes attitude control is needed. The example of LISA-Pathfinder, GOCE and Microscope missions can be quoted.

## II. SPIS liquid ion thruster bundle development and capability

Nonetheless, these technologies present also drawbacks which should be thoroughly studied before using them. One of the main threats to the use of these technologies is the emission of droplets by the thruster. Indeed, these droplets could interact with the satellite body and degrade it. Consequently, droplets dynamic modelling around satellite body is a major topic.

[1] Research Scientist, Department Physics, Instrumentation, Environment, Space (DPHY), marc.villemant@onera.fr

The SPIS software (Spacecraft Plasma Interaction System) was created to model the interaction between spacecraft body and space environment. In order to respond to the need of modelling for droplet/spacecraft body interaction, a new bundle has been developed Liquid Ion Thruster. This bundle introduces a new type of particle: the droplets. The droplets particles are defined by several physical parameters (mass, radius, charge, temperature, droplet material, etc.). A thermal model has been implemented to describe the evolution of droplet temperature, their evaporation and solidification. A contamination model is also implemented to describe attachment and depletion of droplet to and from spacecraft body surface.

## III. First example of SPIS simulation with FEEP and colloid thruster

In this article, we evaluate on an over-simplified test case the level of contamination to expect on LISA due to the use of micro-thrusters. We simulate with SPIS the contamination generated on a dielectric plate by a thruster located nearby and oriented at a grazing incidence relative to the plate. Assuming that no technical reason would lead to have thruster firing toward the spacecraft surface, this is seen as a worst case scenario. The present technical note provides the preliminary study of the contamination issues in the environment of LISA.

### A. Geometry

During this simulation, the satellite body is represented by a plate of aluminium above which stand the thruster (cf. Figure 1). The plate dimensions are 1.5 m x 0.9 m x 5 cm. It is cover by a layer of dielectric Silicate ($SiO_2$). The thruster is assumed to be cylinder with a 5 cm radius located at its centre 55 cm away and 7.5 cm above the silicate covered face. The plate and the thruster are linked by a 1kΩ resistor.

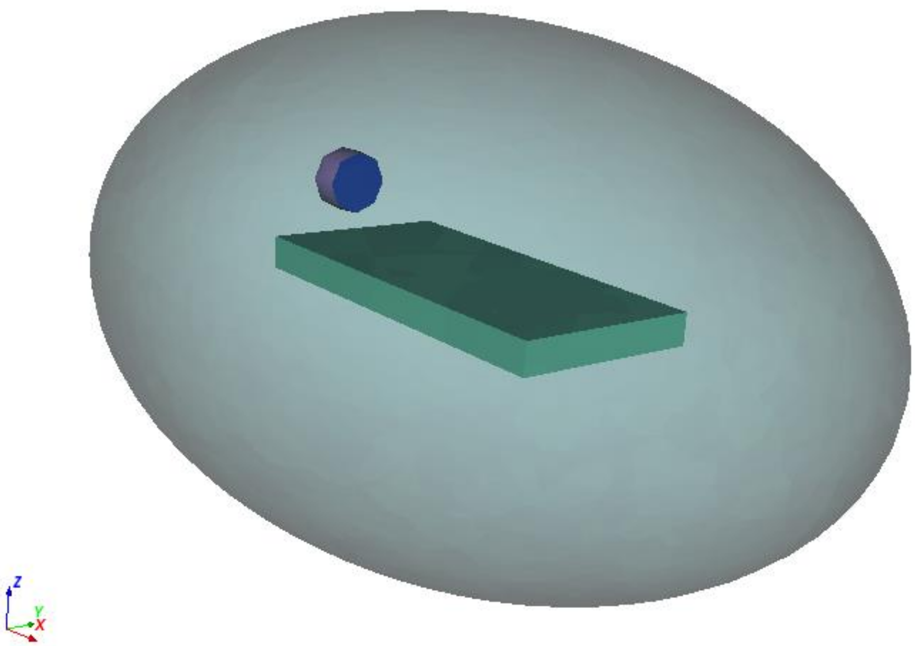


**Figure 1: Contamination test case simulation geometry**

### B. Environment

We simulate environmental conditions corresponding to the solar wind at 1 AU from the sun, in accordance with LISA targeted location. The density and temperature of solar wind electrons and protons are 7 $cm^{-3}$ and 10 eV. The solar wind drift is not modelled in this simple case, the effect of this drift on the contamination being weak and not relevant for a simple model. Both populations are modelled with an analytical Maxwell-Boltzmann distribution.

### C. In-LMIS Indium thruster simulation

We first simulate the contamination due to a FEEP thruster. For the simulation purpose, we choose to define an emitted current of 100µA, we thus data to use with the simulations. The In+ ions are defined by their 100µA current, with a shifted Maxwellian distribution with an average energy of 5.5 keV and a temperature of 1keV, which is consistent with the distribution from [TN1]. The droplet size distribution used in the simulation is the tabulation of that from [TN1] (Figure 2).

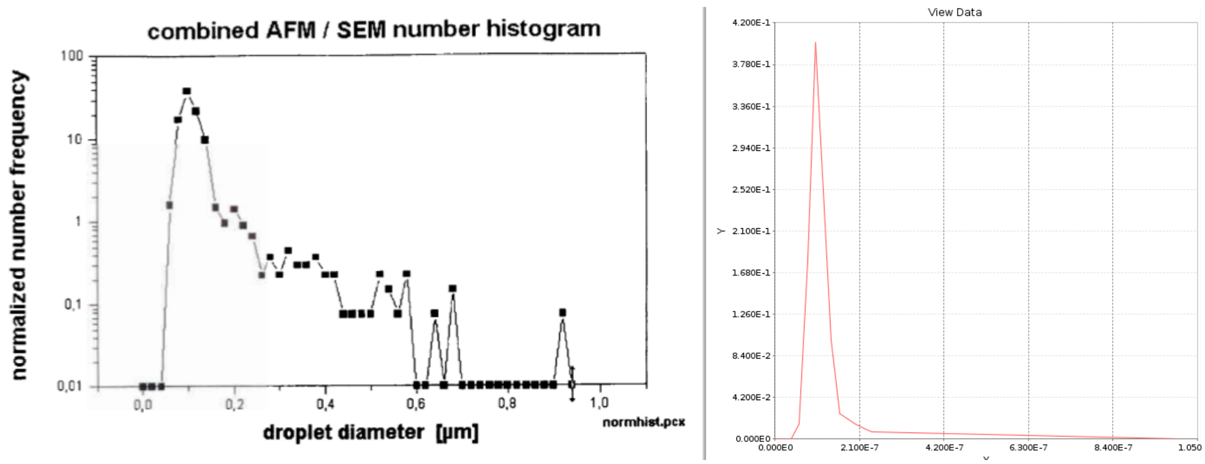


**Figure 2 : Droplet size distribution for a 100µA FEEP thruster. (left) Measured in log scale; (right) simulated in linear scale.**

The dust flux set to $6.10^9$ particles.$m^{-2}$.$s^{-1}$, which represents a total of 4.7 $10^7$ particles per second emitted by the thruster, in accordance with the values from [TN1]. The dust charge is set to 730 e / droplet, which corresponds to the 16 c/kg prescribed by the [TN1].

The simulation setup included the modelling of the contamination by the thruster products, with a sticking coefficient of 1 (i.e. all ions impacting the surface are assumed to stick on it), the droplet deposit (once again with a sticking coefficient of 1), the erosion of the silicate surface and the erosion of the contaminant (indium neutrals).

The simulation was run for 5 seconds of physical time, which is much longer than the time needed to reach the electrostatic equilibrium between the thruster and the plate (Figure 3). The plate potential is -1V in average, but the part of the silicate face closest to the thruster exhaust can reach nearly -6V (Figure 4). The thruster net current is not null, as showed on Figure 3. This implies that the cathode potential is not fully coupled with the environment yet. However, this has no impact on the contamination process, as the relative charging level of the thruster and the plate are correct.

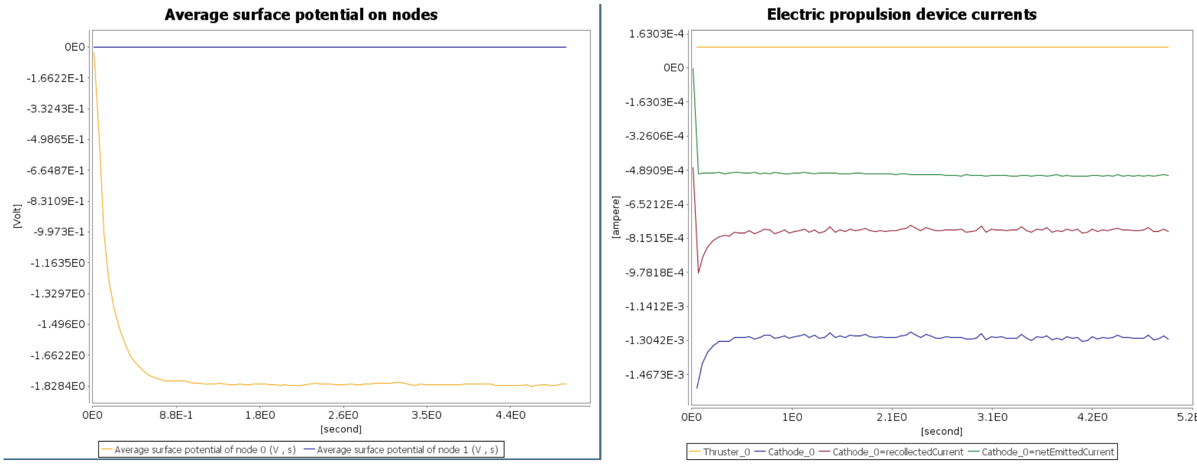


**Figure 3: (left) time evolution of the averaged surface potentials for the thruster (blue curve) and the plate (yellow curve). (right) evolution of the thruster currents: ion current (yellow), cathode net current (green), cathode recollected current (brown) cathode total current (blue).**

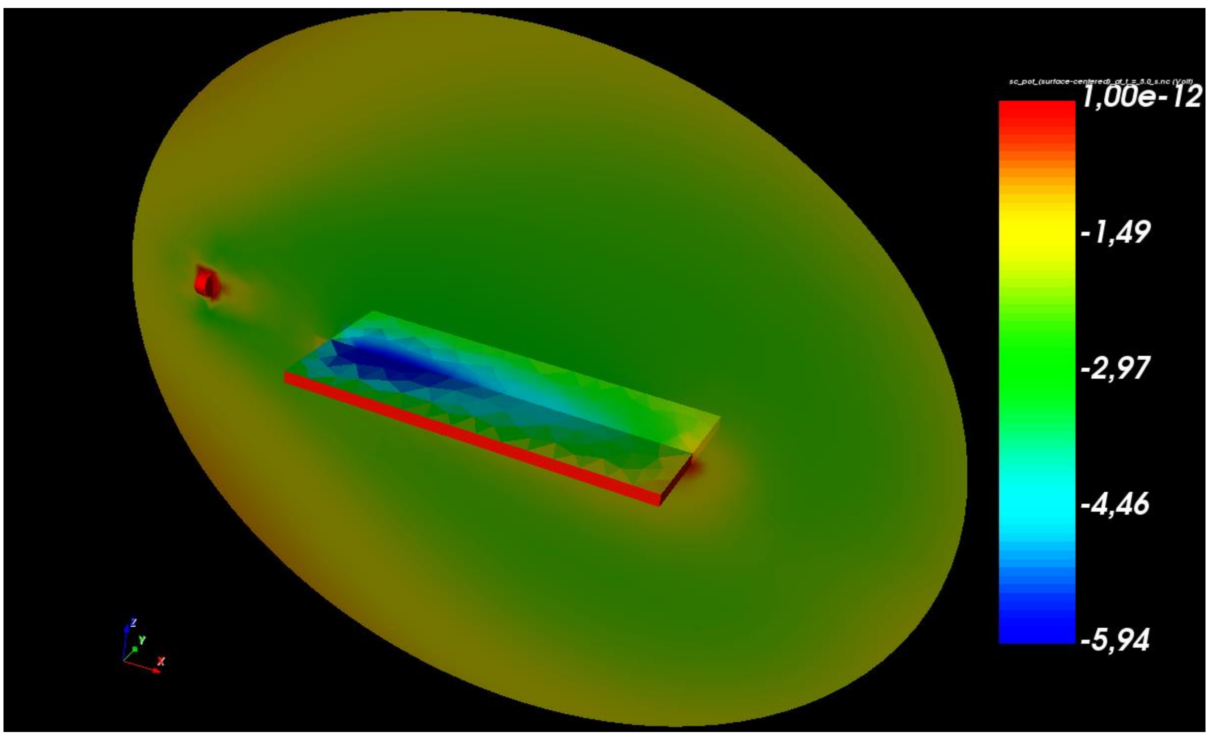


**Figure 4 : Surface and volume potentials. The potential is close to 0, except on the silicate surface that collects more electrons from the thruster. The potentials are negligible compared to the kinetic energy of the indium ions and droplets and do not impact much the contamination.**

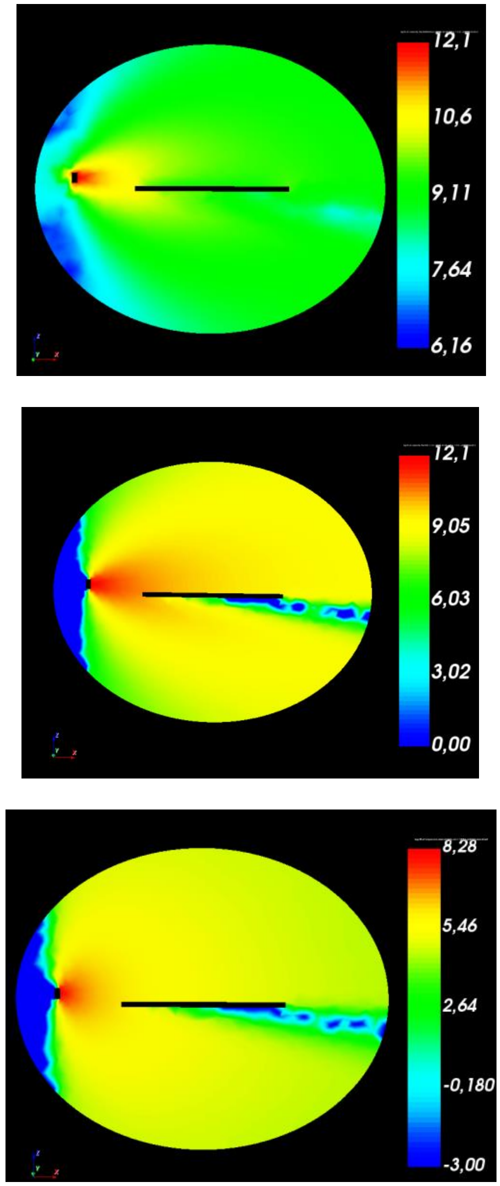


**Figure 5 : densities of cathode electrons (up), thruster ions (middle) and droplets (bottom) in log(m-3).**

Figure 5 shows a 2D cut of the densities of the particles emitted by the thruster. The wake behind the plate can be seen on all populations. The divergence of the droplet beam is larger as we had only had to select a Lambertian distribution for the beam emission pattern.

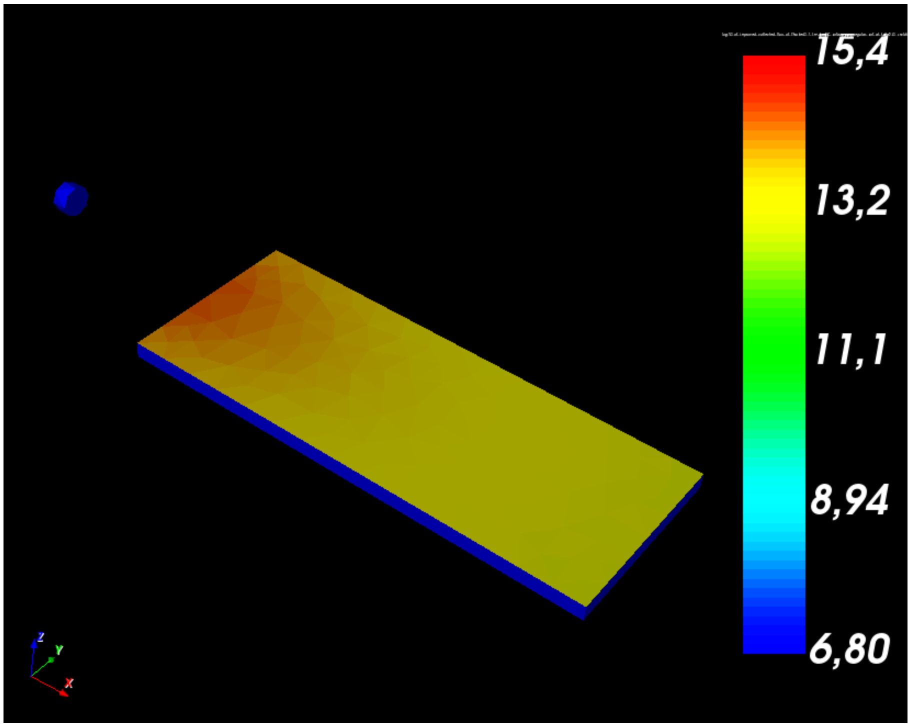


**Figure 6: In+ ion flux on the plate surface [log of ion.m-2.s-1]**

The proximity of the plate relative to the thruster exhaust leads to a large flux of deposited Indium ions (Figure 6), but also to a large erosion of the silicate material covering the plate (Figure 7).

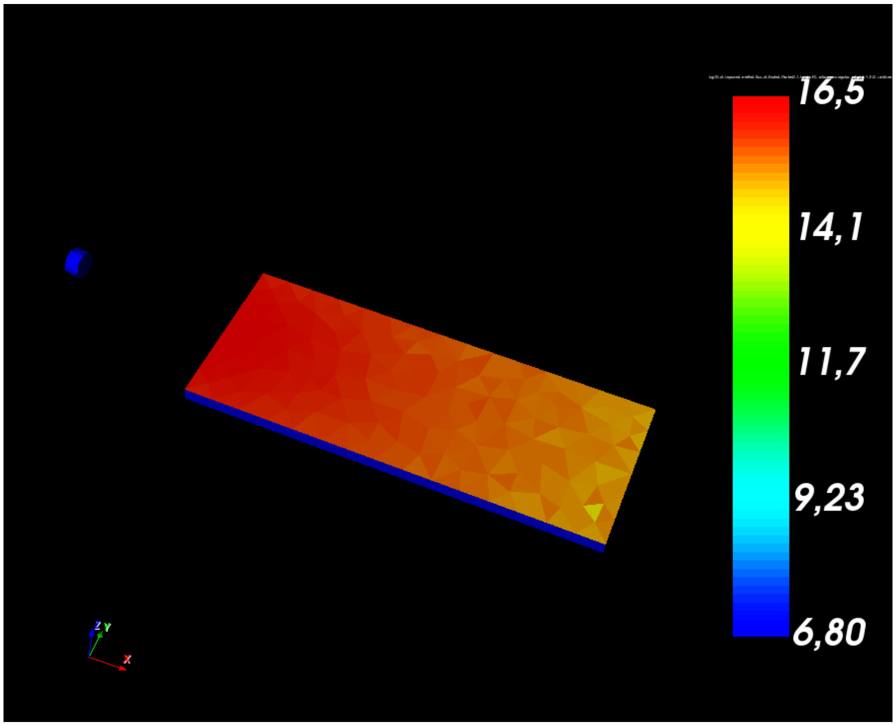


**Figure 7: eroded product flux, in log of molecule.m-2.s-1**

The mass and charge fluxes of deposited droplets are given on Figure 7. These fluxes are stable, indicating that the simulation reached a steady-state. The distribution of the droplet deposit on the plate surface is shown on Figure 8.

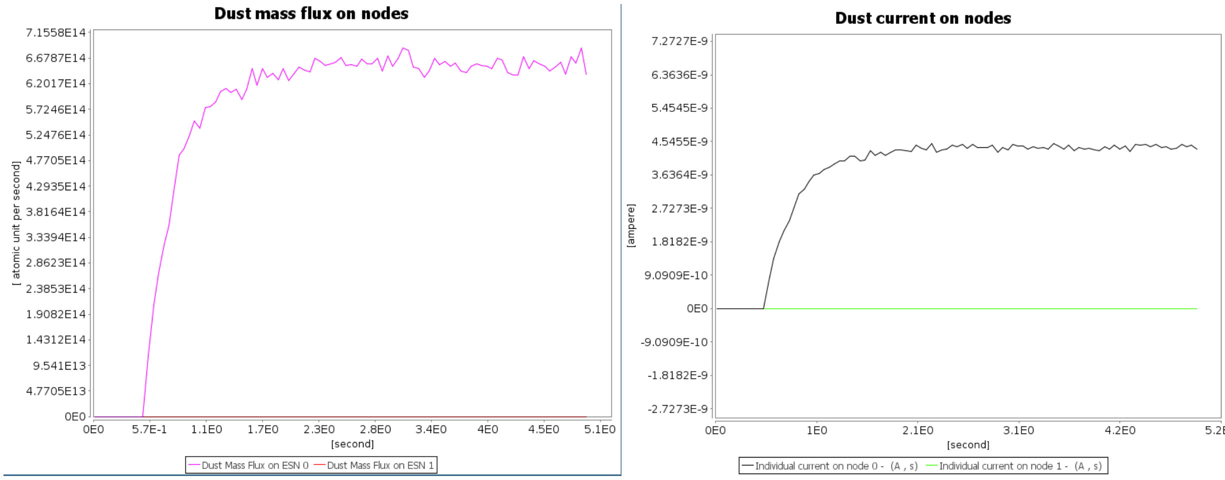


**Figure 8: Droplet mass flux [amu.s-1] and current [A] on the surfaces.**

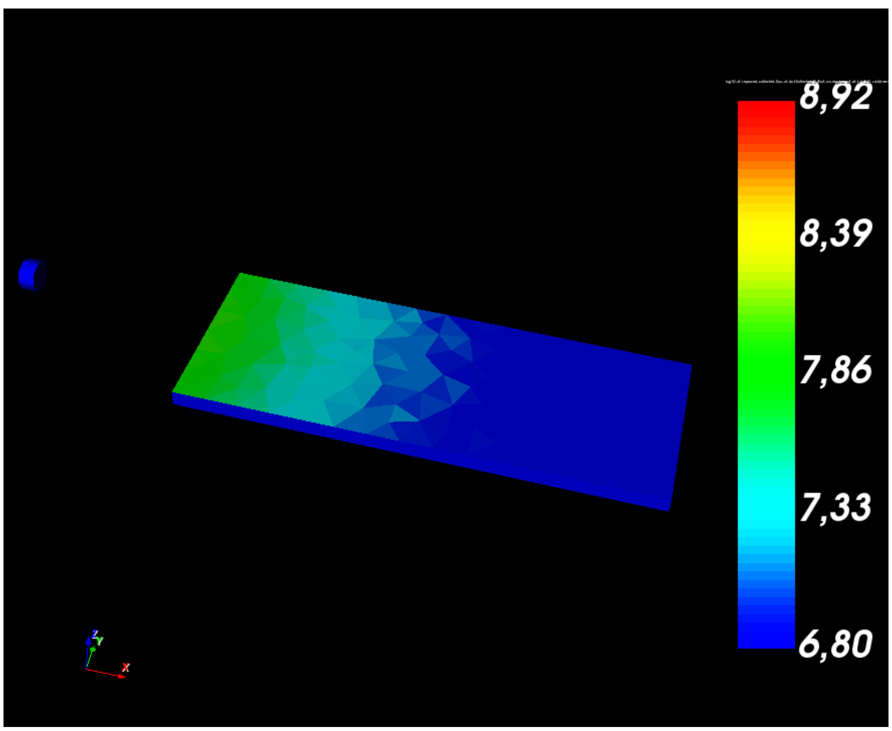


**Figure 9 : flux of droplet deposited on the plate [log of droplet.m-2.s-1]**

### D. ST7-DRS CMNT

We then simulate the contamination due to a colloid thruster. We model the ST7-DR5. The colloid thrusters are primarily controlled by their mass flow. For the purpose of the study, we choose a mass flow of 128 ng/s, corresponding to a volume flux of 100 pL/s.

The total current is set to 350 nA divided between the droplets (60%), EMI-BF4 monomers (10%), dimers (20%) and trimers (10%), according to Figure 30 of the [TN1]. The characteristics of the ions emitted by the thruster are displayed on Figure 10, together with a summary of the populations simulated.

The droplet size is set to 22 nm according, and the droplet flux is set to $10^{11}$ droplets.m$^{-2}$.s, or 1.75 $10^{9}$ droplet/s in order to be consistent with the mass flow. The individual charge per droplet is set to 1320 e/droplet in order to be consistent with the expected droplet current.

**Figure 10 : summaries of the thruster and plasma species characteristics.**

The simulation is run for a longer duration than for the FEEP simulation (50 seconds), the convergence time being longer due to the smaller current. Nonetheless, the surface potentials show a clear convergence of the simulation (Figure 11). The thruster currents show a large noise on the cathode net current. This is probably due to the importance of the droplet population in the simulation. Each droplet carrying a large charge, they introduce a large noise on the currents.

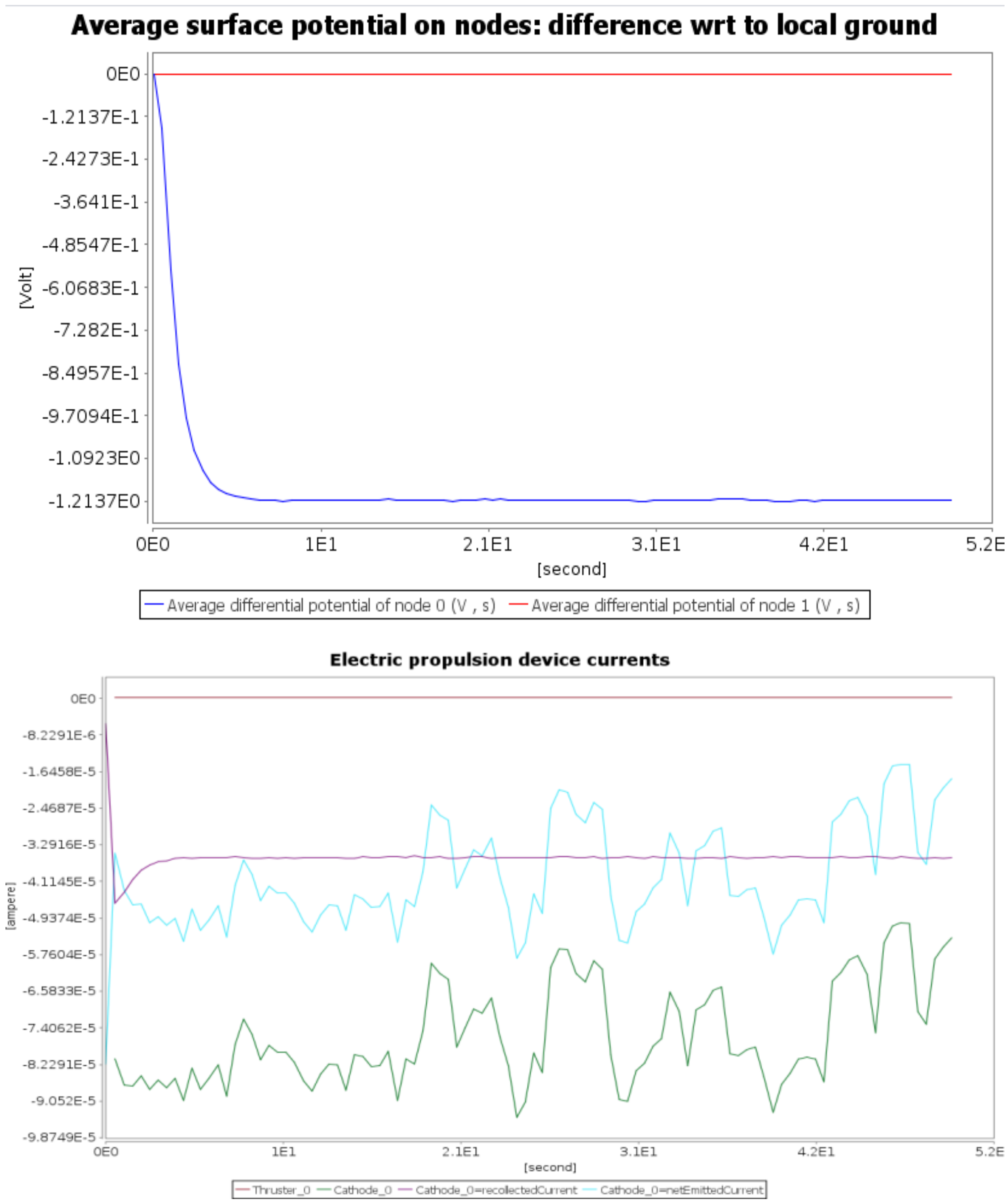


**Figure 11 : (left) time evolution of the averaged surface potentials for the thruster (red curve) and the plate (blue curve). (right) evolution of the thruster currents: ion current (brown), cathode net current (blue), cathode recollected current (purple) cathode total current (green).**

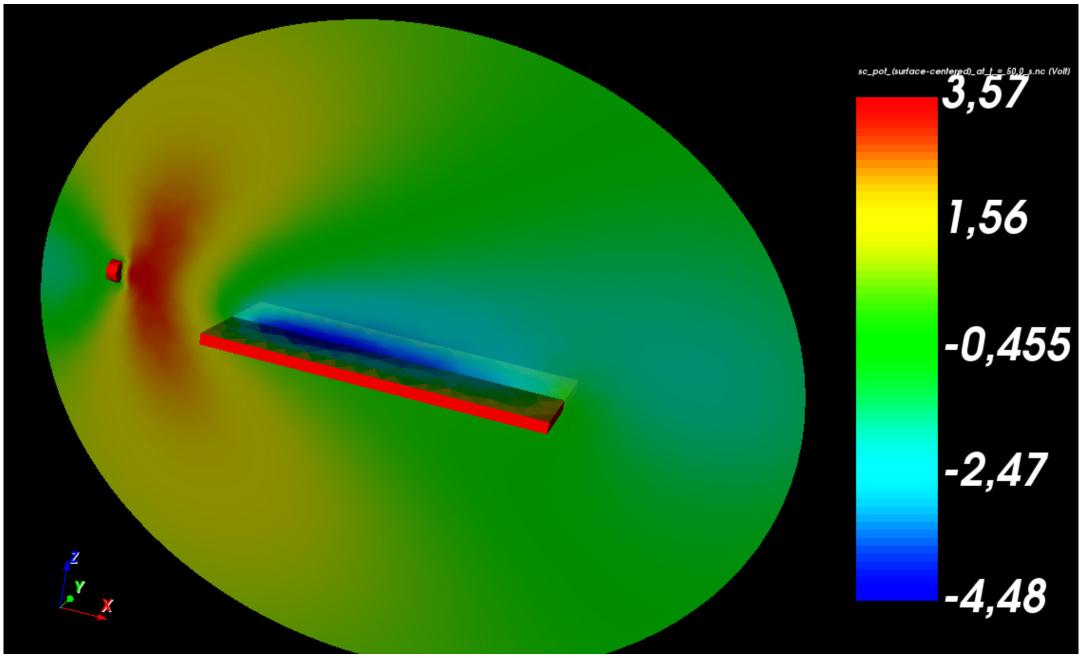


**Figure 12 : Surface and volume potentials. The potential is close to 0, except on the silicate surface that collects more electrons from the thruster. The potentials are negligible compared to the kinetic energy of the indium ions and droplets and do not impact much the contamination.**

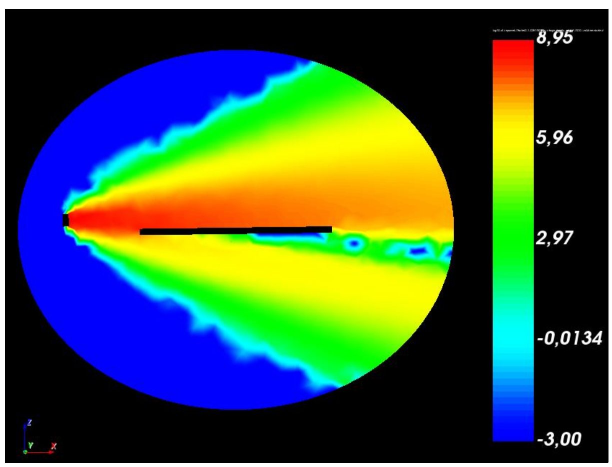

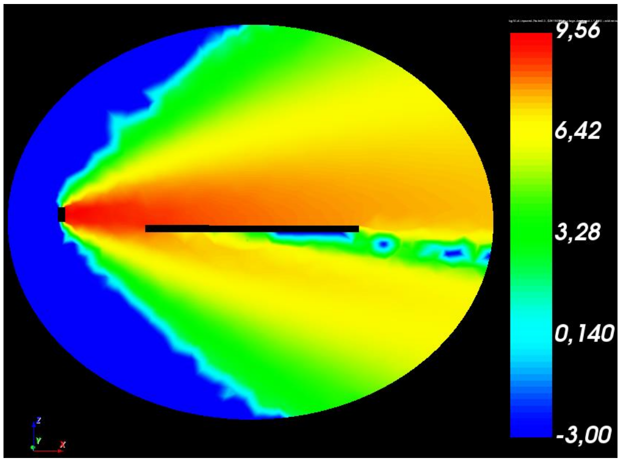
9,56
6,42
3,28
0,140
-3,00

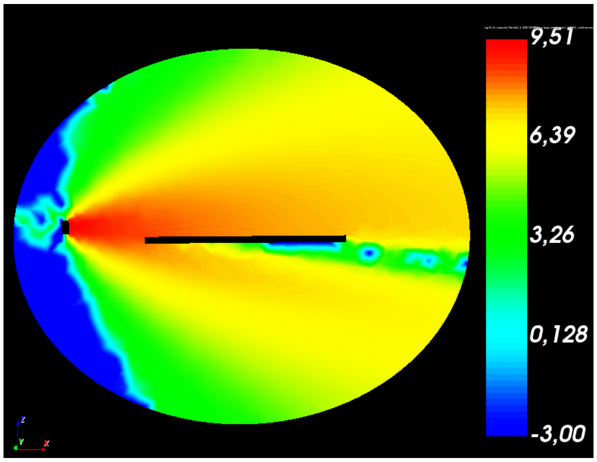
9,51
6,39
3,26
0,128
-3,00

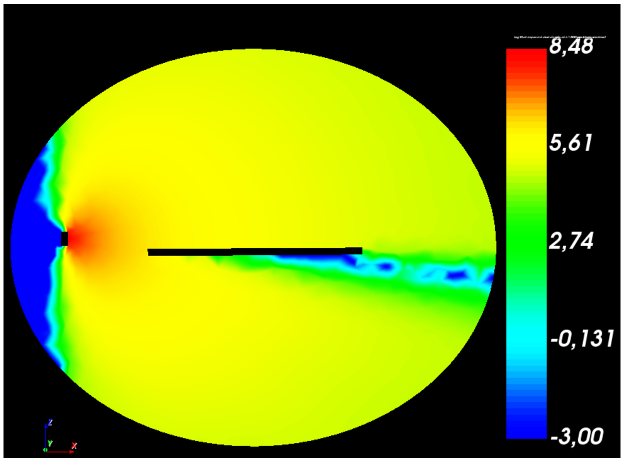
8,48
5,61
2,74
-0,131
-3,00

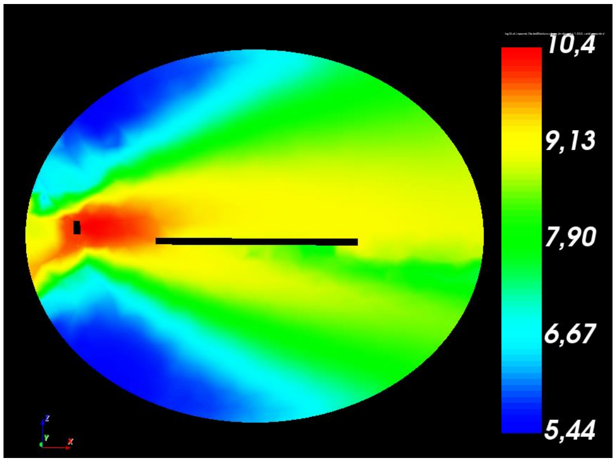


**Figure 13 : From top to bottom : densities of (EMI-BF4)+, (EMI-BF4)2+, (EMI-BF4)3+, EMI-BF4 droplets and cathode electrons**

The electric potential in volume (Figure 12) and on the plate surface is very similar to that obtained with the FEEP thruster, except for the positive potential at the exhaust of the thruster which is due to the large divergence of the droplet beam and to the fact that the cathode electrons do not neutralize well the droplets. In reality, droplets have a much narrower divergence angle, so that this structure may not exist. Concerning the effect of the cathode electrons, it must be noted that when field emission neutralizers are used instead of hollow cathodes, the neutralizer electrons do not neutralize the charge in volume (they only equilibrate the current), so that the electrons model we use may not be far from a real case, even though it was imposed by the software constraints.

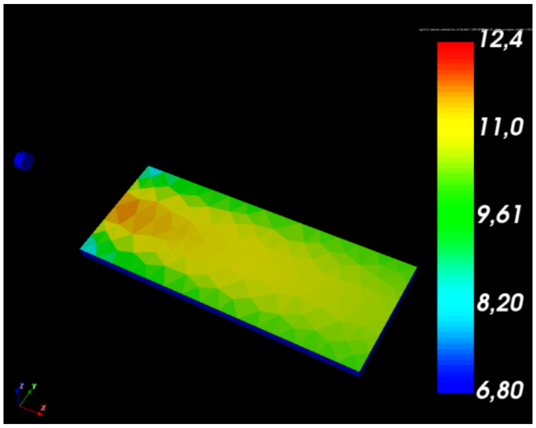


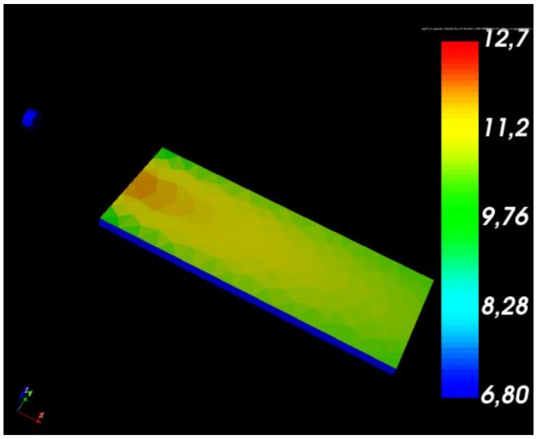

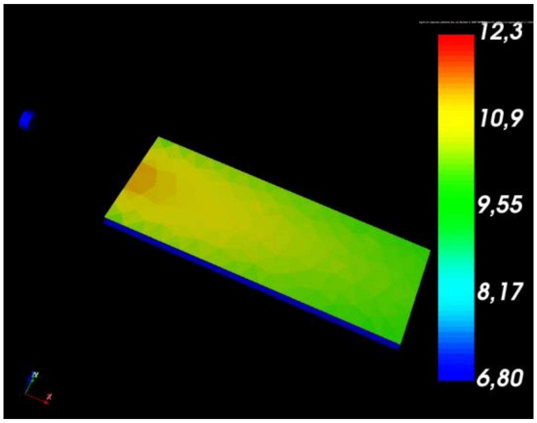


**Figure 14 : Fluxes of EMI-BF4+ monomers (top), dimers (middle) and trimers (bottom). These ions are singly ionized.**

As for the FEEP case, the proximity of the thruster exhaust leads to a large deposition of colloids ions on the plate, the deposition rates are very similar for monomers, dimers and trimers. Contrary to the indium case, we do not discuss the possible erosion of the silicate material by the ions, since the erosion model in SPIS is not adapted to model to possible erosion of material due to the impact of large molecules.

The evolutions of the mass and charge fluxes of deposited droplets are given on Figure 15. These fluxes are stable, indicating that the simulation reached a steady-state. The distribution of the droplet deposit on the plate surface is shown on Figure 16.

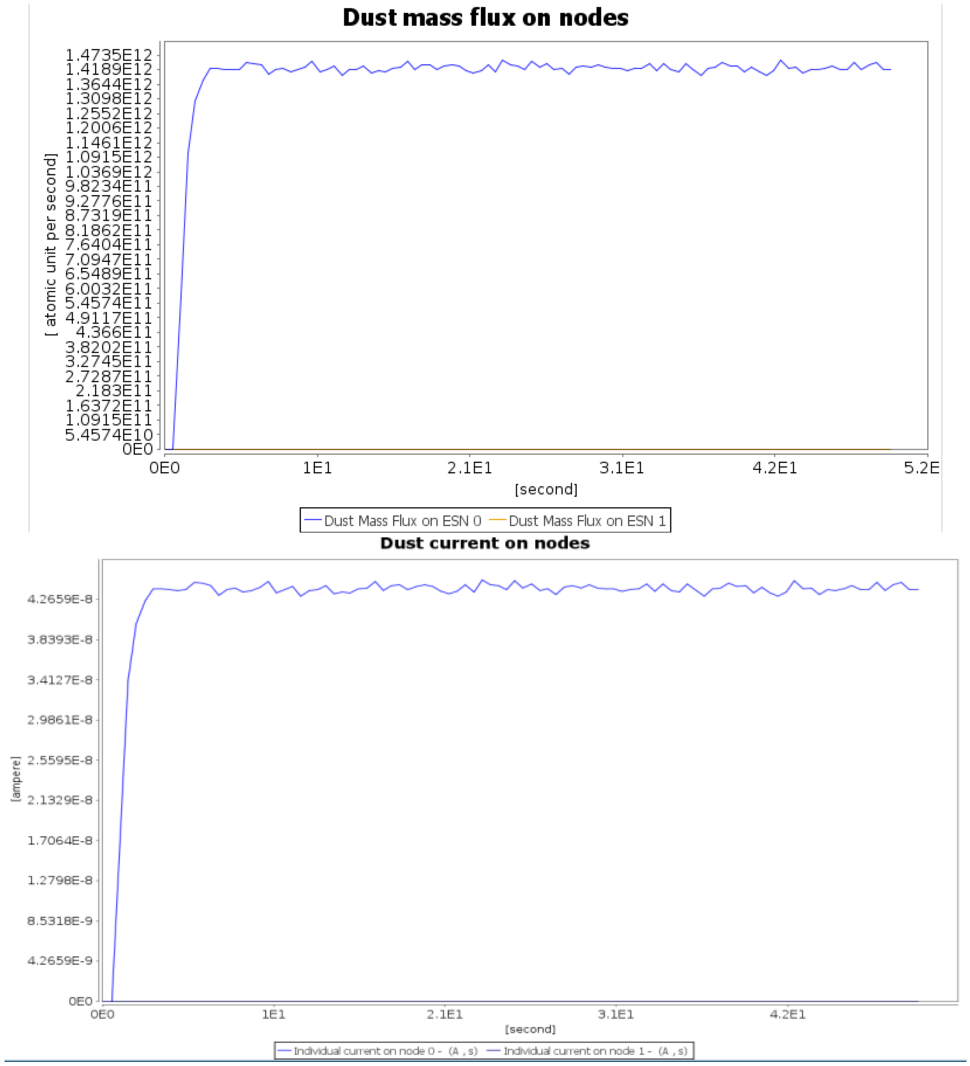


**Figure 15 : Droplet mass flux [amu.s-1] and current [A] on the surfaces.**

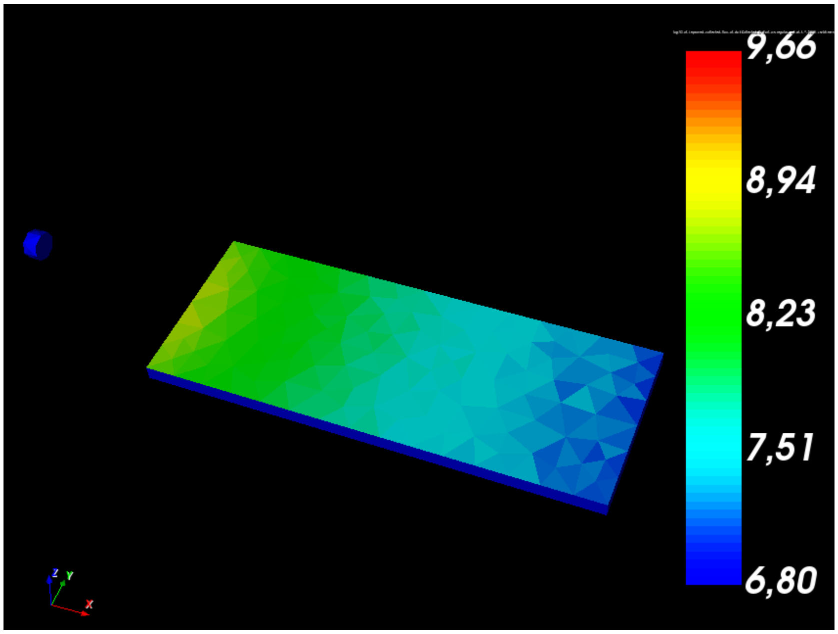

**Figure 16 : flux of droplet deposited on the plate [log of droplet.m-2.s-1]**

## IV. Conclusion and further SPIS development

In this article, the recent development of SPIS software about droplet dynamic, charging, thermal model, surface contamination and depletion were presented. It has been shown that the current development will allow to carry out modelling studies on droplets / spacecraft body interaction. This will allow designing and optimizing satellites architecture when they use FEEP or colloids technologies.

Future SPIS development will focus on contamination and depletion model development as well as describing more precisely the way droplets deposit on spacecraft body surfaces (e.g. by defining the droplets spreading of droplets on surfaces).

## References

[1] R. W. Hockney and J. W. Eastwood, *Computer Simulation Using Particles*. CRC Press, 1988.

[2] C. K. Birdsall and A. B. Langdon, *Plasma Physics via Computer Simulation*. CRC Press, 2004.

[3] V. Vahedi and M. Surendra, "A Monte Carlo collision model for the particle-in-cell method: applications to argon and oxygen discharges," *Computer Physics Communications*, vol. 87, no. 1, pp. 179–198, May 1995.

[4] J. Pierron, C. Inguimbert, M. Belhaj, T. Gineste, J. Puech, and M. Raine, "Electron emission yield for low energy electrons: Monte Carlo simulation and experimental comparison for Al, Ag, and Si," *Journal of Applied Physics*, vol. 121, no. 21, p. 215107, Jun. 2017.

[5] D. Sydorenko, "Particle-in-cell simulations of electron dynamics in low pressure discharges with magnetic fields," University of Saskatchewan Saskatoon, 2006.

[6] D. Sydorenko, A. Smolyakov, I. Kaganovich, and Y. Raitses, "Modification of electron velocity distribution in bounded plasmas by secondary electron emission," *Plasma Science, IEEE Transactions on*, vol. 34, pp. 815–824, Jul. 2006.

[7] J. R. M. Vaughan, "A new formula for secondary emission yield," *IEEE Transactions on Electron Devices*, vol. 36, no. 9, pp. 1963–1967, Sep. 1989.

[8] M. S. Chung and T. E. Everhart, "Simple calculation of energy distribution of low-energy secondary electrons emitted from metals under electron bombardment," *Journal of Applied Physics*, vol. 45, no. 2, pp. 707–709, Feb. 1974.

[9] A. Jablonski, "Angular distribution of elastic electron backscattering from surfaces: determination of the electron inelastic mean free path," *J. Phys. D: Appl. Phys.*, vol. 47, no. 5, p. 055301, 2014.

[10] S. Barral, K. Makowski, Z. Peradzyński, N. Gascon, and M. Dudeck, "Wall material effects in stationary plasma thrusters. II. Near-wall and in-wall conductivity," *Physics of Plasmas (1994-present)*, vol. 10, no. 10, pp. 4137–4152, Oct. 2003.

[11] A. Domínguez-Vázquez, F. Taccogna, and E. Ahedo, "Particle modeling of radial electron dynamics in a controlled discharge of a Hall thruster," *Plasma Sources Sci. Technol.*, vol. 27, no. 6, p. 064006, Jun. 2018.